



Article

Phytocannabinoids Reduce Inflammation of Primed Macrophages and Enteric Glial Cells: An In Vitro Study

Gal Cohen, Ofer Gover [†] and Betty Schwartz ^{*,†}

Department of Biochemistry Food Science and Nutrition, The Robert H. Smith Faculty of Agriculture, Food and Environment, The Hebrew University of Jerusalem, Herzl Street 229, Rehovot 7610001, Israel; galgalita124@gmail.com (G.C.); ofer.gover@mail.huji.ac.il (O.G.)

* Correspondence: betty.schwartz@mail.huji.ac.il

[†] These authors contributed equally to this work.

Abstract: Intestinal inflammation is mediated by a subset of cells populating the intestine, such as enteric glial cells (EGC) and macrophages. Different studies indicate that phytocannabinoids could play a possible role in the treatment of inflammatory bowel disease (IBD) by relieving the symptoms involved in the disease. Phytocannabinoids act through the endocannabinoid system, which is distributed throughout the mammalian body in the cells of the immune system and in the intestinal cells. Our in vitro study analyzed the putative anti-inflammatory effect of nine selected pure cannabinoids in J774A1 macrophage cells and EGCs triggered to undergo inflammation with lipopolysaccharide (LPS). The anti-inflammatory effect of several phytocannabinoids was measured by their ability to reduce TNF α transcription and translation in J774A1 macrophages and to diminish S100B and GFAP secretion and transcription in EGCs. Our results demonstrate that THC at the lower concentrations tested exerted the most effective anti-inflammatory effect in both J774A1 macrophages and EGCs compared to the other phytocannabinoids tested herein. We then performed RNA-seq analysis of EGCs exposed to LPS in the presence or absence of THC or THC-COOH. Transcriptomic analysis of these EGCs revealed 23 differentially expressed genes (DEG) compared to the treatment with only LPS. Pretreatment with THC resulted in 26 DEG, and pretreatment with THC-COOH resulted in 25 DEG. To evaluate which biological pathways were affected by the different phytocannabinoid treatments, we used the Ingenuity platform. We show that THC treatment affects the mTOR and RAR signaling pathway, while THC-COOH mainly affects the IL6 signaling pathway.

Keywords: phytocannabinoids; J774A1 M1 macrophages; enteric glial cells



Citation: Cohen, G.; Gover, O.; Schwartz, B. Phytocannabinoids Reduce Inflammation of Primed Macrophages and Enteric Glial Cells: An In Vitro Study. *Int. J. Mol. Sci.* **2023**, *24*, 14628. <https://doi.org/10.3390/ijms241914628>

Academic Editors: Susanne M. Krug and Lidia V. Boldyreva

Received: 8 August 2023

Revised: 20 September 2023

Accepted: 25 September 2023

Published: 27 September 2023



Copyright: © 2023 by the authors. Licensee MDPI, Basel, Switzerland. This article is an open access article distributed under the terms and conditions of the Creative Commons Attribution (CC BY) license (<https://creativecommons.org/licenses/by/4.0/>).

1. Introduction

Intestinal inflammation is mediated by a subset of cells populating the intestine [1,2]. Macrophages are key players in the innate immune system, and are involved in phagocytosis, antigen presentation, and secretion of various cytokines, chemokines, and growth factors that protect the body from infection [3]. In the integral part of the normal intestinal tissues, macrophages are well-established in the lamina propria and in Peyer's patches, where they function as immune effector cells against any pathogenic attack [4]. In the presence of inflammatory stimuli, macrophages polarize toward the pro-inflammatory M1 phenotype that produces high levels of inflammatory cytokines and chemokines in order to eliminate pathogens [4]. The exposure of macrophages to lipopolysaccharide (LPS) or Tumor necrosis factor alpha (TNF- α) induced their differentiation to the M1 phenotype [5]. Typically, M1 macrophages secrete toxic cytokines, such as TNF- α , IL-1 β , IL-6, IL-12, IL-18, IL-23, nitric oxide, and reactive oxygen species (ROS). In addition, M1 macrophages decrease the stimulation of the anti-inflammatory cytokine IL-10 [6]. In contrast, wound healing environment promotes macrophage polarization to the anti-inflammatory M2 state with increased production of anti-inflammatory cytokines, leading to alleviating inflammation, tissue repair, and remodeling [7,8]. Emerging evidence has shown that recruitment of

a large number of M1 inflammatory macrophages to inflamed tissues associated with high production of pro-inflammatory cytokines contributes to inflammation and tissue damage in inflammatory diseases [9]. Macrophages exhibit a particularly vigorous response to LPS, a surface component of most Gram-negative bacteria, and TNF- α in response to inflammation or injury. The dysfunction of the mucosal immune response in IBD is characterized by abnormalities in both the innate and adaptive immune systems [10]. The final common pathway of this dysregulated immune activation is abundant infiltration of immune cells, such as macrophages and monocytes, in the intestinal mucosa [11–13].

The gastrointestinal tract differs from all other peripheral organs in that it includes an extensive enteric nervous system (ENS), differing from all other peripheral organs. The ENS is characterized by the presence of neurons and enteric glial cells (EGCs), which are arranged into interconnected ganglia distributed between the plexuses. There is evidence indicating that inflammatory diseases of the gut are characterized by changes affecting enteric glial cells [14,15]. EGCs are activated by exogenous stimuli that lead to over-release of neurotrophins, growth factors, and cytokines that, in turn, recruit infiltrating immune cells such as macrophages, neutrophils, and mast cells into the colonic mucosa [16–18]. In fact, EGCs exert a key role in the maintenance of gut homeostasis through cooperating with surrounding cells. Specifically, EGCs assure the correct trophism of neurons in the ENS [1,18], protect neurons from oxidative stress [19], control epithelial barrier functions by reducing epithelial permeability, and actively participate in the course of intestinal inflammation acting as the first defensive line of the ENS [1,17]. Enteric glial cells have also gained a particular interest for IBD pathogenic processes since they morphologically and functionality resemble astrocytes, which maintain homeostasis in the central nervous system [20]. The response to different insults, such as inflammation and infection [21,22], is manifested by expressing glial fibrillary acidic protein (GFAP) and S100 calcium-binding protein B (S100B) [10,23]. In the disease state, inflammation can convert EGCs to a “reactive EGC phenotype” characterized by over-release of neurotrophins, growth factors, and cytokines that, in turn, recruit infiltrating immune cells such as macrophages, neutrophils, and mast cells in the colonic mucosa [17,24]. In this pathological condition, increased GFAP and S100B protein expression from EGCs have also been observed. These two proteins provide reliable biomarkers of glial activation in the intestinal tissue [23,25].

The endocannabinoid system (ECS) comprises endogenous cannabinoids (endocannabinoids (eCBs)), cannabinoid receptors, and proteins that transport, synthesize, and degrade eCBs. Most components of the ECS are multifunctional. Thus, rather than being a discrete system, the ECS influences, and is influenced by, many other signaling pathways. This is especially important to consider when assessing the effects of ECS-targeting drugs [26]. The actions of most phytocannabinoids is mediated via receptors that are part of the ECS, through agonistic and antagonistic actions at specific receptors sites [26,27] and in varying degree of affinity [28]. The best-known receptors of the ECS are cannabinoid receptor 1 (CB1R) and cannabinoid receptor 2 (CB2R). Both receptors are G-protein coupled receptors (GPCR) that activate intracellular signaling [29]. For example, the mitogen-activated protein kinase (MAPK) pathway results from G-protein-coupled receptors activation [30], such as the resulting CB1 stimulation [27,31]. CB1Rs are found mainly on neurons, in the brain, and in the spinal cord, and they are expressed by some astrocytes [32,33]. In addition, CB1Rs are expressed in many peripheral organs and tissues, including in the gastrointestinal tract [34,35], in the enteric nervous system [36], in the healthy colonic epithelium, in the gut smooth muscles, and in the submucosal myenteric plexus [37].

CB2 receptors are primarily expressed in cells of immune origin [38], including microglia [39], though they may also be expressed in neurons [39], particularly in pathological statuses [33]. Indeed, there is markedly more mRNA for CB2R than CB1R in the immune system [38]. CB2R are also present in epithelial and immune cells from the gastrointestinal tract [40] and, in contrast to CB1 receptors, CB2 receptors are highly expressed in macrophages and in colonic epithelium tissue taken from IBD patients [37]. In fact, increased epithelial CB2 receptor expression in human inflammatory bowel disease tissue

implies an immunomodulatory role that may affect mucosal immunity. The endocannabinoid system has been demonstrated to be activated in several conditions, including inflamed intestine in mice, and, thus, expresses an increased amount of endocannabinoid receptors [41].

Our aim in this study was to analyze the putative anti-inflammatory effect of nine selected pure cannabinoids *in vitro* in J774A1 macrophages cells and enteric glial cells (EGCs) triggered to undergo inflammation with lipopolysaccharide (LPS). The anti-inflammatory effect of the phytocannabinoids was measured by their ability to reduce TNF α transcription and translation in J774A1 macrophages and to diminish S100B and GFAP secretion and transcription in EGCs.

2. Results

2.1. Effects of Phytocannabinoids on Inflammation in Murine Macrophages and EGC

The detection of TNF α levels provided us with an acceptable criterion to evaluate the extent of inflammation. The maximal response to LPS elicitation of J77A1 cells was detected by the level of secretion of TNF α and measured after treatment with LPS (0.05 μ g/mL) for 4 h (Figure S1A). Treatment with dexamethasone at a concentration of 5 μ M (Figure S1B) provided us the most suitable control indicator of reduction of inflammatory response in J77A1 cells. All further analyses were performed with 0.05 μ g/mL of LPS for 4 h for secretion of TNF α and 0.05 μ g/mL of LPS for 1 h for gene expression (Figure S1).

EGCs play a fundamental role in gut maintenance and inflammation. During intestinal inflammation, EGCs enter reactive gliosis and overexpress S100B protein, a molecule that plays a pivotal role in the downstream signaling process of EGC inflammation [16]. Furthermore, it has been shown that EGCs express CB2 receptors [42]. Quantification of cellular S100B protein was performed by ELISA. Sparstolonin B (Ssnb) is a polyphenol which inhibits TLR4 activation by blocking the binding of TLR4 to MyD88 (an important mediator of almost all the TLR downstream signaling), thereby suppressing Nuclear factor- κ B (NF- κ B) [43,44]. Treatment with Ssnb at a concentration of 10 μ g/L provided us the most suitable control indicator of reduction of inflammatory response in EGCs. Afterwards, EGCs were incubated with 1 μ g/mL LPS for 24 h. EGCs express not only S100B, but also express high levels GFAP [45] upon inflammatory stimulation.

All cannabinoids were assayed for cytotoxicity using the MTT method [46] on J774A1, and concentrations that did not reduce cell viability were selected for further analysis (Figure S2). For CBGA and CBDA, all concentrations tested reduced cell viability by at least 50% and, hence, were not evaluated further (Figure S2F,G).

2.1.1. THC

The putative cytotoxic effect of Delta-9-tetrahydrocannabinol (THC) was evaluated by (3-(4,5-dimethylthiazol-2-yl)-2,5-diphenyltetrazolium bromide) tetrazolium reduction assay (MTT). We demonstrate that THC was not toxic to the cells at concentrations up to 10 μ g/mL (Figure S2A). THC induced the greatest effect on reducing TNF α secretion at either 0.1 or 0.05 μ g/mL (Figure 1A). This reduction was comparable to the effect of dexamethasone. Above these concentrations, THC increased TNF α secretion to levels equal to (0.1–1 μ g/mL) or above (5–10 μ g/mL) treatment with LPS (Figure 1A). The extent of reduction of secretion did not mirror the effects measured on gene expression (Figure S4A).

Pretreatment of EGCs with 0.05 μ g/mL and 0.1 μ g/mL THC led to a significant reduction in inflammation by lowering S100B protein levels (Figure 1B) and GFAP expression levels (Figure 1C). In EGC, a dose-dependent reduction in inflammatory markers was observed.

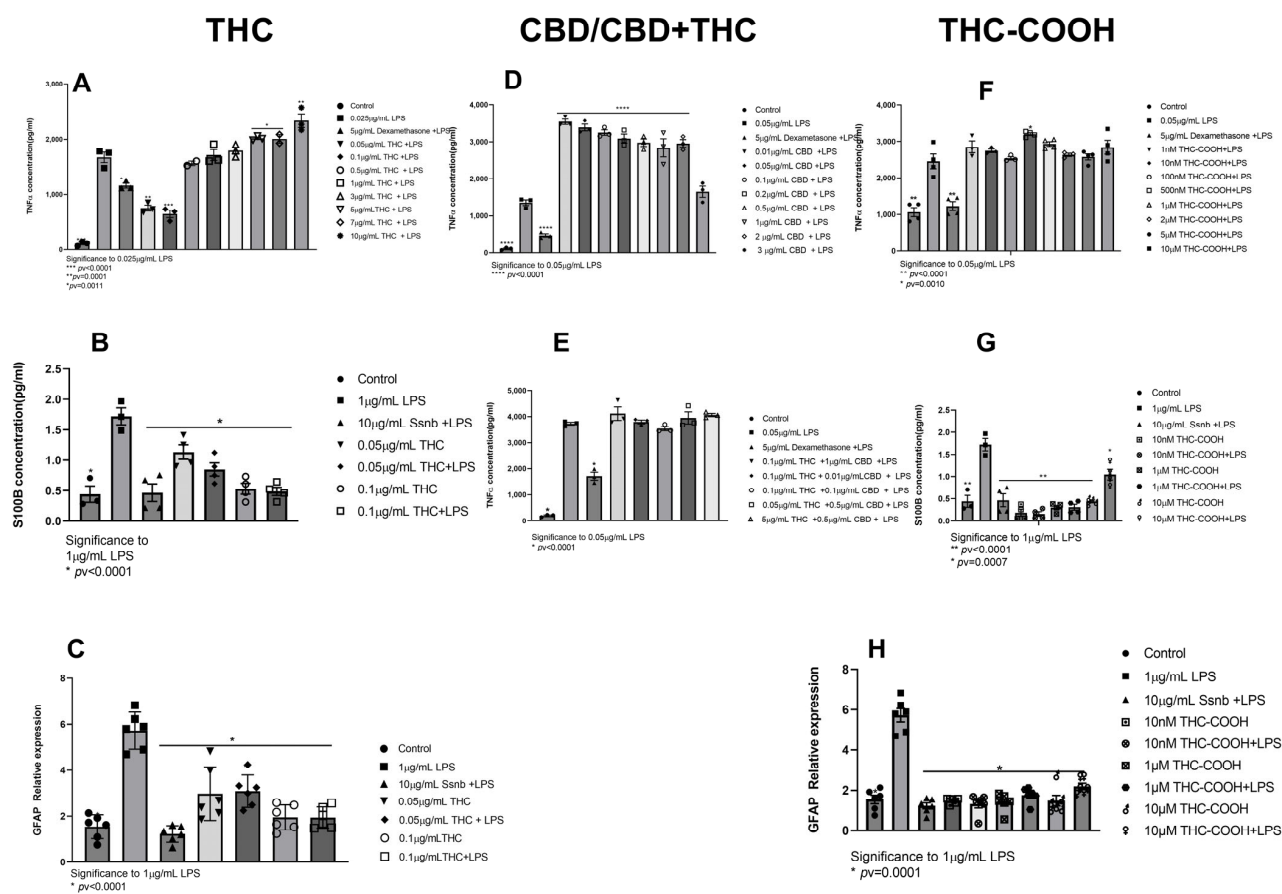


Figure 1. Pretreatment of J774A1 and EGC with THC (A–C), CBD (D,E), and THC-COOH (F–H) for 1 h and then incubation with LPS 0.05 μ g/mL and 1 μ g/mL for J774A1 and EGC, respectively, for an additional 24 h. Control represents J774A1/EGCs without treatment, 0.05/1 μ g/mL LPS represents the positive control for J774A1/EGCs, and 5 μ g/mL Dexamethasone and 10 μ g/mL Ssnb treatment represents the negative control for J774A1 or EGC, respectively. (A) Secretion of TNF α by J774A1 cells treated with 0.05–10 μ g/mL THC and 0.05 μ g/mL LPS. (B) Secretion of S100B from EGCs pretreated with 0.05 and 0.1 μ g/mL THC with and w/o 1 μ g/mL LPS. (C) Expression of GFAP from EGCs pretreated with 0.05 and 0.1 μ g/mL THC with and w/o 1 μ g/mL LPS. (D) TNF α secretion from J774A1 pretreated with 0.01–3 μ g/mL CBD with 0.05 μ g/mL LPS. (E) TNF α secretion from J774A1 pretreated with a combination of THC + CBD and 0.05 μ g/mL LPS. (F) TNF α secretion from J774A1 pretreated with 1 nM–10 μ M THC-COOH with 0.05 μ g/mL LPS. (G) Secretion of S100B from EGCs pretreated with 1 nM–10 μ M THC-COOH with 0.05 μ g/mL LPS. (H) Expression of GFAP from EGCs pretreated with 1 nM–10 μ M THC-COOH with 0.05 μ g/mL LPS. $n = 3$ for all J774A1 TNF α secretion, $N = 4$ for EGC S100B secretion, $N = 6$ for GFAP expression. All samples were compared to positive LPS control using Dunnett’s multiple comparison test.

2.1.2. CBD

Cannabidiol (CBD) is the second most abundant phytocannabinoid with non-psychoactive effects, which makes it well tolerated by consumers compared to THC [47]. CBD was not toxic to the cells up to 3 μ g/mL (Figure S1B). Treatment J77A1 macrophages with CBD concentrations under the cytotoxicity level induced increased secretion of TNF α (Figure 1D). Furthermore, the combination of THC and CBD abolished THC’s anti-inflammatory effect (Figure 1D).

2.1.3. THC-COOH

Metabolism of THC occurs mainly in the liver by microsomal hydroxylation and oxidation catalyzed by enzymes of the cytochrome P450 (CYP) complex [48]. The first prod-

uct is 11-Hydroxy Δ^9 -tetrahydrocannabinol (11-OH-THC), while 11-Nor-9-carboxy- Δ^9 -tetrahydrocannabinol (11-THC-COOH or THC-COOH) is the final product. THC-COOH is not psychoactive and possesses anti-inflammatory and analgesic properties by mechanisms similar to those of nonsteroidal anti-inflammatory drugs [49]. Concentrations of THC-COOH above 10 μ M were toxic to J774A1 cells (Figure S2E) and, above 100 μ M, to EGC (Figure S3B). Most of the concentrations of THC-COOH (1 nM, 10 nM, 100 nM, 1 μ M, 2 μ M, 5 μ M, and 10 μ M) that we tested did not exert a significant effect on TNF- α secretion. However, 500 nM increased TNF- α in those cells (Figure 1F). Concentrations from 1 nm to 10 μ M significantly reduced S100B secretion and expression (Figures 1G and S4D) and GFAP expression (Figure 1H).

2.1.4. THCA

In the plant trichome, THC is stored in its acidic form, Δ^9 -tetrahydrocannabinol acid (THCA) [50]. THCA is devoid of psychotropic effects [51]. THCA needs to undergo decarboxylation to THC to produce psychotic effects; this decarboxylation is spontaneous and requires heat [27]. We show in cell viability experiments that THCA is not cytotoxic to J774A1 or to EGC up to 10 μ M (Figures S2C and S3A). In concentrations below 10 μ M, THCA increased secretion of TNF α in J774A1 cells compared to 0.05 μ g/mL LPS without pretreatment (Figure 2A). In concentrations of 0.1–10 μ M, THCA reduced S100B secretion and expression (Figures 2B and S4C) and GFAP expression (Figure 2C). THCA alone did not elevate S100B secretion or GFAP expression (Figure 2B,C).

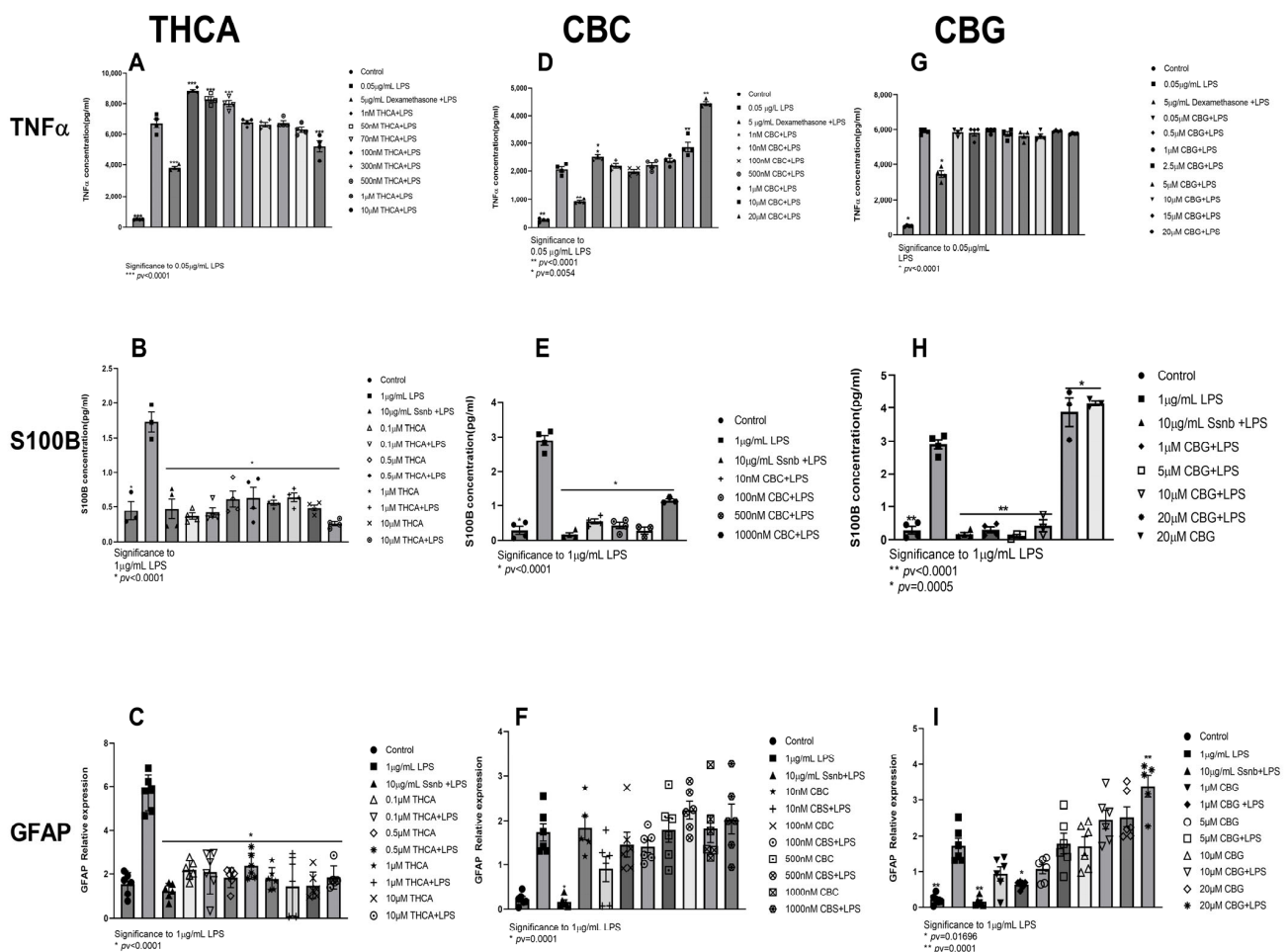


Figure 2. Pretreatment of J774A1 and EGC with THCA (A–C), CBC (D–F), and CBG (G–I) for 1 h and then incubation with LPS 0.05 μ g/mL and 1 μ g/mL for J774A1 and EGC for 4 h. Control represents

J774A1/EGCs without treatment, 0.05/1 $\mu\text{g}/\text{mL}$ LPS represents the positive control for J774A1/EGCs and 5 $\mu\text{g}/\text{mL}$ Dexamethasone and 10 $\mu\text{g}/\text{mL}$ Ssnb treatment represents the negative control for J774A1 or EGC, respectively. (A) Secretion of $\text{TNF}\alpha$ by J774A1 cells treated with 1 nM–10 μM THCA and 0.05 $\mu\text{g}/\text{mL}$ LPS. (B) Secretion of S100B from EGCs pretreated with 1 nM–10 μM THCA with and w/o 1 $\mu\text{g}/\text{mL}$ LPS. (C) Expression of GFAP from EGCs pretreated 1 nM–10 μM THCA and 0.05 $\mu\text{g}/\text{mL}$ with and w/o 1 $\mu\text{g}/\text{mL}$ LPS. (D) $\text{TNF}\alpha$ secretion from J774A1 pretreated with 1 nM–20 μM CBC with 0.05 $\mu\text{g}/\text{mL}$ LPS. (E) Secretion of S100B from EGCs pretreated with a 1 nM–20 μM CBC with 1 $\mu\text{g}/\text{mL}$ LPS. (F) expression of GFAP from EGCs pretreated with 1 nM–20 μM CBC with 1 $\mu\text{g}/\text{mL}$ LPS. (G) $\text{TNF}\alpha$ secretion from J774A1 pretreated with 0.05–20 μM CBG with 0.05 $\mu\text{g}/\text{mL}$ LPS. (H) Secretion of S100B from EGCs pretreated with a 1–20 μM CBG with 1 $\mu\text{g}/\text{mL}$ LPS. (I) Expression of GFAP from EGCs pretreated with 1–20 μM CBG with or w/o 1 $\mu\text{g}/\text{mL}$ LPS, $N = 3$ for all J774A1 $\text{TNF}\alpha$ secretion, $n = 4$ for EGC S100B secretion, $N = 6$ for GFAP expression. All samples were compared to positive LPS control using Dunnett's multiple comparison test.

2.1.5. CBC and CBG

Pretreatment with CBC and CBG did not exert any cytotoxic effect on J77A1 cells below 10 μM and 20 μM , respectively (Figure S2H,I). CBC treatment of J774A1 macrophages showed a U-shaped curve where 1 nM, 10 μM , and 20 μM significantly elevated $\text{TNF}\alpha$ secretion compared to LPS control, and concentrations between 10 nM and 1 μM were insignificant related to control (Figure 2D). Pretreatment with 10 nM–1 μM CBC significantly reduced S100B secretion and expression to the same levels as Ssnb (Figures 2E and S4F). Concentrations of 10 nM, 100 nM, 500 nM, and 1 μM CBC did not exert any effect on GFAP expression (Figure 2F).

CBG did not exert any significant effect on $\text{TNF}\alpha$ secretion in comparison to the positive control (0.05 $\mu\text{g}/\text{mL}$ LPS) over the whole range of CBG concentrations tested (0.05–20 μM CBG) (Figure 2G).

CBG treatment induced an anti-inflammatory effect in EGCs at 1–10 μM for S100B secretion (Figure 2H). However, the effect on secretion differs from the effect on relative expression of S100B (Figures 2H and S4E). A discrepancy between S100B expression and translation in EGCs after treatment with 20 μM CBG (Figures 2H and S4E) was seen where it increased S100B secretion yet showed decreased transcription. Only 1 μM of CBG significantly reduced GFAP expression, whereas a dose-dependent increase in GFAP expression was seen with and without LPS (Figure 2I).

2.1.6. THCv

Δ^9 -Tetrahydrocannabivarin (THCV) is described as a phytocannabinoid belonging to one of the minor phytocannabinoids. The name "minor phytocannabinoids" has been used to define phytocannabinoids different from Δ^9 -THC, CBD, CBG, and CBC. THCv decreases signs of inflammation and pain in an acute inflammation model in mice partly via CB1 and/or CB2 receptor activation [52]. We show, for J77A1 macrophages, that THCv is not cytotoxic below 15 nM (Figure S2D). THCv treatment of J774A1 cells showed significant increases in $\text{TNF}\alpha$ secretion from cells at concentrations of 0.2 nM, 0.5 nM, 1 nM, and 3 nM compared to the 0.05 $\mu\text{g}/\text{mL}$ LPS group (Figure 3). Although it is not significant, 5 nM, 7 nM, 10 nM, and 15 nM showed an increase in $\text{TNF}\alpha$ secretion compared to J774A1 cells treated with 0.05 $\mu\text{g}/\text{mL}$ LPS (Figure 3).

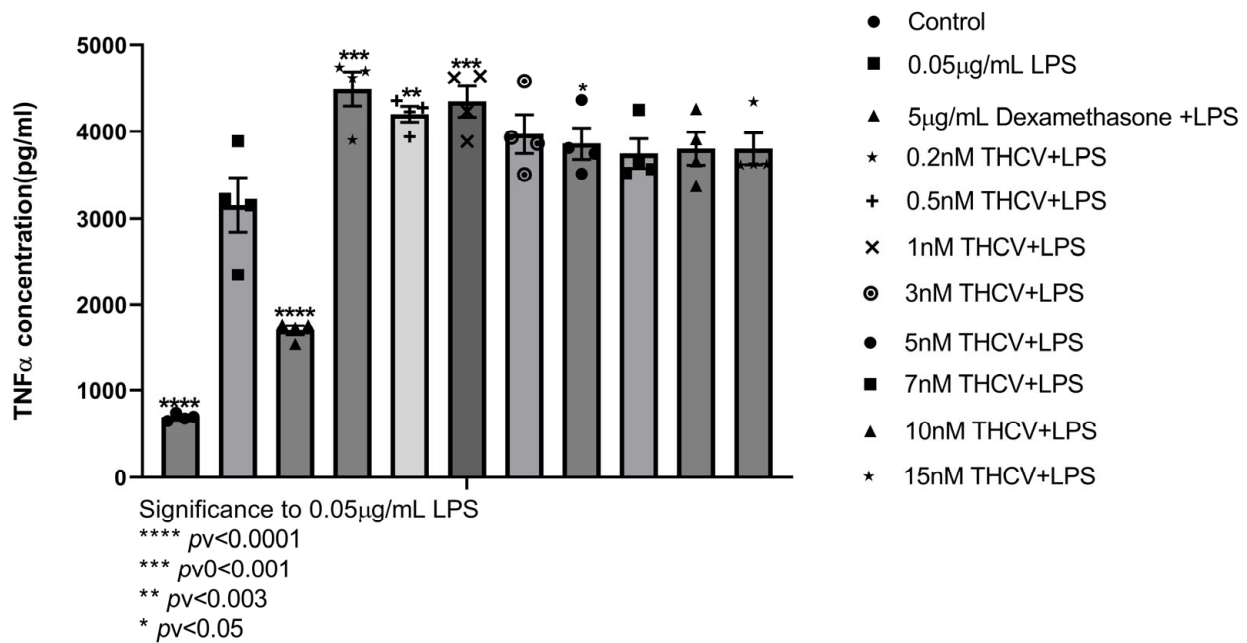


Figure 3. Pretreatment of J77A1 macrophages with increasing concentrations. J77A1 cells were pretreated with 0.2–15 nM THCV for 1 h and then incubated with 0.05 μ g/L of LPS for 4 h. Control represents J77A1 cells without treatment, 0.05 μ g/mL LPS represents the positive control, and 5 μ g/mL Dexamethasone treatment represents the negative control. $n = 4$. All samples were compared to positive LPS control using Dunnett's multiple comparison test.

2.2. RNA Sequencing Analysis

EGCs were treated for 1 h with 0.1 μ g/mL of THC or 10 nM of THC-COOH, after which 1 μ g/mL of LPS was added for 4 h. Additionally, a positive control of 1 μ g/mL LPS and negative control cells were used. Transcriptomic analysis revealed 23 differentially expressed genes (DEG) (fold change >1.6 , $p < 0.05$) in the control vs LPS (10 upregulated and 13 downregulated), 26 DEG THC + LPS vs LPS (10 upregulated and 16 downregulated) and 25 DEGs when comparing THC-COOH + LPS vs LPS (16 upregulated and 9 downregulated) (Figure 4). Pretreatment with THC before LPS resulted in downregulation of the apoptosis related genes *mob1a* ($p < 0.05$, -1.7 FC) [53] and *ptma* ($p < 0.05$, -2 FC). THC downregulated *adm* ($p < 0.05$, -1.6 FC), a gene that is upregulated in inflamed neurons, and antagonists to *adm* inhibit the release of nNOS and macrophage recruitment [54]. *Ap1s3* was upregulated by pretreatment with THC ($p < 0.05$, 3.5 FC). Knockout of *ap1s3* in keratinocytes results in upregulation of IL1 and TNF α [55]. IL1 is a strong activator of IBD [56,57]. Oxidative stress genes were also affected by THC with downregulation of *gpx8* ($p < 0.05$, -2 FC) and upregulation of *oplah* ($p < 0.05$, 3 FC).

THC-COOH is the final metabolite of THC metabolism in the liver. Pretreatment of THC-COOH resulted in upregulated genes relating to cellular metabolism, including *cox6c*, *cox7b*, and *gbe1* (Figure 4). THC-COOH upregulated *psma2*, a component of the 20S subunit. Knockdown of this gene results in reduced immune response in human lung cells [58].

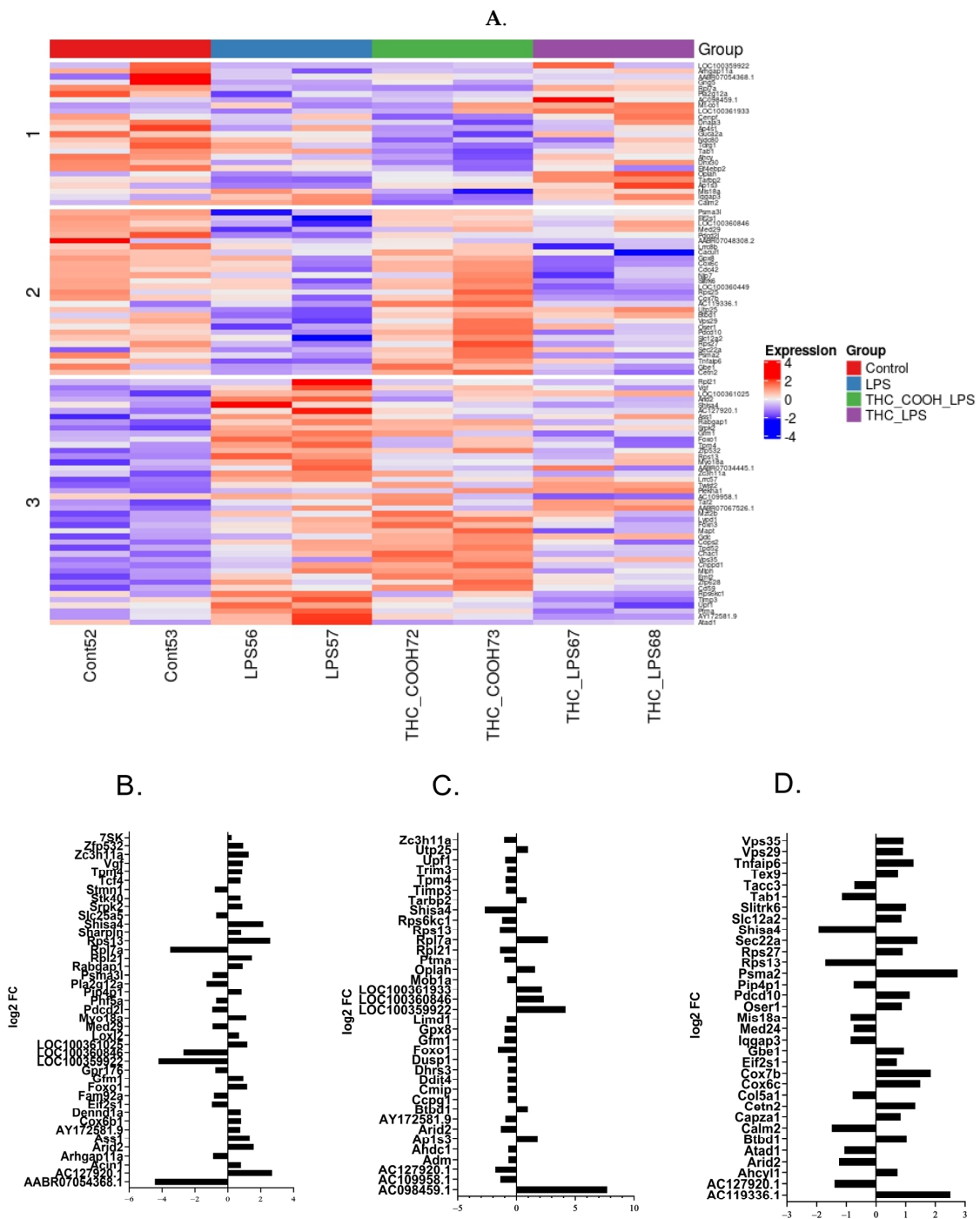


Figure 4. Differentially expressed genes (DEG) in enteric glial cells (EGC): (A): Differential expression of all groups: (B) Non-treated cell compared to cells treated with LPS 1 µg/mL for 24 h. (C): 1 h pretreatment with 0.1 µg/mL THC before 24 h of LPS compared to only LPS 1 µg/mL. (D): 1 h pretreatment of 10 nM of THC-COOH before 24 h of LP compared to only LPS 1 µg/mL. n = 2.

Pathway Enrichment Analysis

To evaluate the biological pathways affected by the different pretreatments, we used the IPA platform ($p < 0.05$). Addition of LPS affected 34 canonical pathways ($-\log(p\text{-value}) > 1$) (Figure 5). The 4 major pathways ($-\log(p\text{-value})$ 2.88–3.78) were related to: oxidative phosphorylation ($-\log(p\text{-value})$ 3.78), mitochondrial dysfunction ($-\log(p\text{-value})$ 3.51), EIF2 signaling ($-\log(p\text{-value})$ 2.88), and HER-2 signaling ($-\log(p\text{-value})$ 2.88). Downregulation of *cox6c* ($\log_2\text{FoldChange}$ -2.46) and *cox7b* ($\log_2\text{FoldChange}$ -2.63) and

upregulation of *mt-co1* (log2FoldChange 1.97) results in changes in oxidative phosphorylation, mitochondrial dysfunction, and HER-2 signaling. Pretreatment with THC for 1 h also affected the Elf2 signaling pathway through downregulation of *gm15489*, *mt-rnr1*, and *rpl21*; however, *rpl7a* was upregulated. The most affected pathway by pretreatment with THC was the mTOR pathway ($-\log_{10}p$ 3.96) Figure 5). This manifested through downregulation of four genes (*ddit4*, *gm15483*, *mt-rnr1*, *rps6kc1*). The only pathway to show mild downregulation was the retinoic acid receptor (RAR) (zScore -2). Interestingly, the final metabolite of THC, THC-COOH, affected different pathways when compared to THC. The carboxylated metabolite elicited changes in IL-6 signaling (*tab1* $-\log_{10}FC -2.2$, *tnfaip6* $-\log_{10}FC 2.4$) and iNos signaling (*Tab1* $-\log_{10}FC -2.2$); both are canonical pathways related to inflammation. In general, carboxylated THC affected fewer pathways compared to THC above the threshold of 1.3 (Figure 5B,C). IPA analysis identifies genetic networks that are affected by the DEG regardless of the direction of the expression change. A total of 0.1 $\mu\text{g/mL}$ LPS affected the cell cycle and cell death network through 11 DEGs (Figure 5D). Pretreatment with THC affected the 17 DEGs of the proteasome network (Figure 5E). The main network to be affected by pretreatment of THC-COOH was related to cell death and survival (Figure 5F).

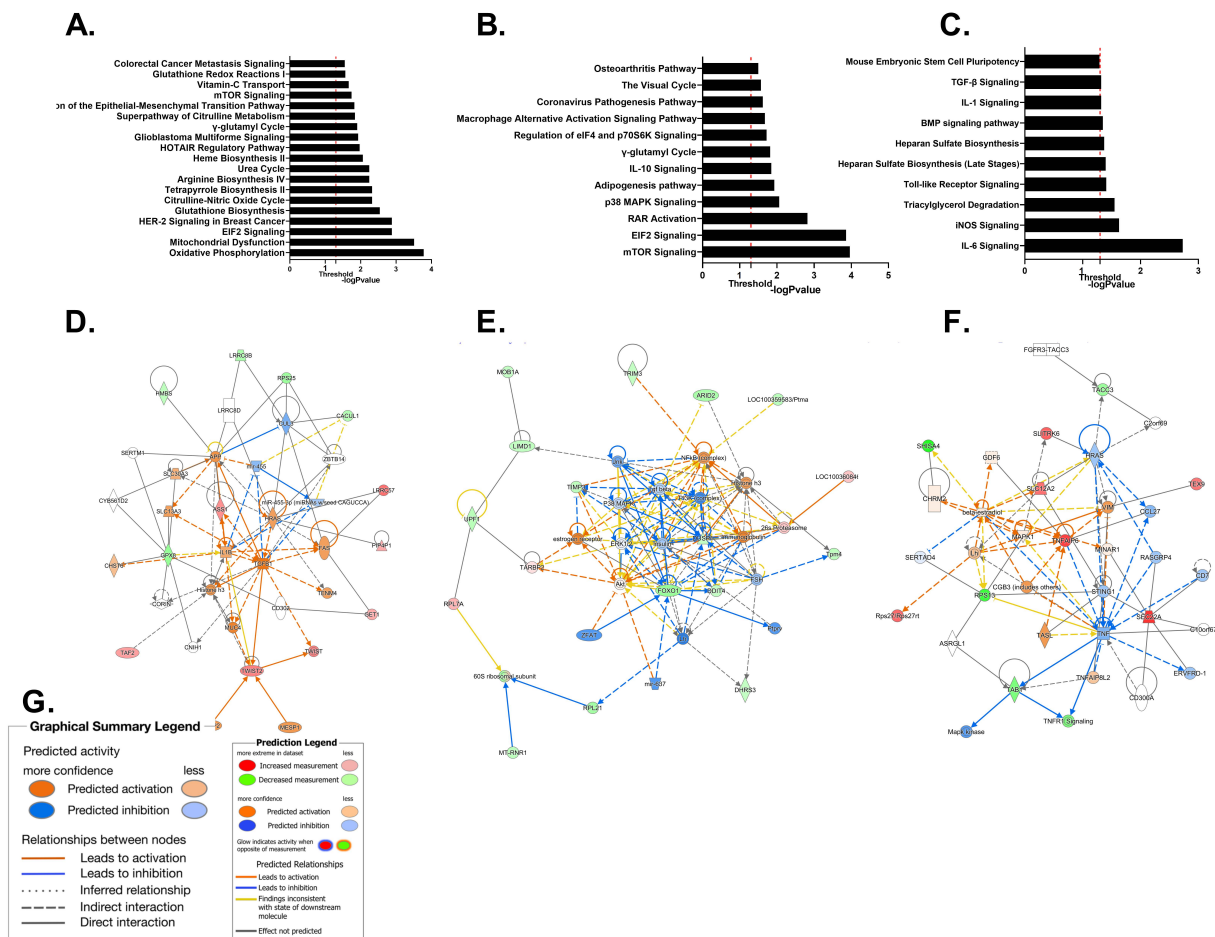


Figure 5. EGCs were either untreated or incubated with 1 $\mu\text{g/mL}$ of LPS (A,D). In treatment groups, cells were pretreated for 1 h with 0.1 $\mu\text{g/mL}$ of THC (B,E) or 10 nM of THC-COOH (C,F). IPA was conducted on three experimental groups. Pathway enrichment (A–C), networks showing most hits (D–F). Pathway analysis of (A) LPS vs untreated cells, (B) Cells pretreated for 1 h with 0.1 $\mu\text{g/mL}$ of THC, (C) cells pretreated for 1 h with 10 nM of THC-COOH. Threshold 1.3 $-\log_{10}p$. (D) Cell cycle and cell death network affected by addition of LPS to untreated cells. (E) Proteasome network effected by pretreatment of THC. (F) Cell cycle and cell death network affected by pretreatment of cells with THC-COOH. (G) Legend for network. $n = 2$.

3. Discussion

In this study, we aimed to perform an in-depth assessment of the putative anti-inflammatory effects of both major and minor phytocannabinoids on macrophages and enteric glial cells. Macrophages are resident cells of almost every tissue in the body and provide key orchestrators of chronic inflammatory disorders. Macrophages have been reported to play a role in the pathological progression of UC (Ulcerative Colitis) disease in comparison with other leukocytes [59]. The glial cells in the gut represent the morphological and functional equivalent of astrocytes and microglia in the central nervous system, and they play essential roles as regulators of intestinal homeostasis [60,61]. Although no CBr have been detected in EGCs, there is mounting evidence on the effects of modulation of EGCs by the ECS [62]. During intestinal inflammatory reaction, EGCs release glial markers such as S100B and GFAP. Altered expression of S100B and GFAP has been reported in several intestinal inflammatory disorders in humans, such as inflammatory bowel disease [16,45], celiac disease [17], and postoperative colitis [40]. However, EGCs were not in the focus of cannabinoid research [62].

Our results show that THC significantly reduced TNF α secretion preferentially at low concentrations 0.05–0.5 $\mu\text{g}/\text{mL}$, whereas, above 0.55 $\mu\text{g}/\text{mL}$, TNF α secretion was increased. At 5–105 $\mu\text{g}/\text{mL}$, secretion was above the effect of 0.5 $\mu\text{g}/\text{mL}$ LPS, showing an additive effect of THC on TNF α secretion. This is in accordance with the known biphasic effect of THC [63,64]. Becker et al. showed a reduction in cytotoxic T cells and T-bet + TH1 cells in THC and THC + CBD mice subjected to dextran sodium sulfate (DSS) and 2,4,6-trinitrobenzenesulphonic acid (TNBS) induced UC [65] compared to vehicle control and CBD. Yakhtin et al. showed that activated peritoneal macrophages treated with THC and THC extract have reduced NO, IL6, TNF α , CXCL2, and G-CSF compared to vehicle control [66]. These data point to the advantage of using low or even ultralow doses of THC, in accordance with the reversal of cognitive impairment in old mice and spatial memory tests in old female mice [67,68]. Transcription of TNF α was not affected by pretreatment with THC; this was evident from RTqPCR (Figure S4A) and transcriptomics. This is inline with other reports showing the instability of TNF α mRNA vs protein [69,70]. Pretreatment of EGC with low concentrations of THC markedly reduced S100B secretion and expression as well as GFAP expression (Figure 1B,C). Taken together, these results show the significant immunosuppressive effect exerted by low doses of THC in our *in vitro* model.

We demonstrate herein that CBD augmented the secretion of TNF α in all concentrations tested except for 3 $\mu\text{g}/\text{mL}$, where it was the same as 0.5 $\mu\text{g}/\text{mL}$ LPS control (Figure 1D). CBD has been used for the treatment of inflammation and other comorbidities [71,72]. Our results may be due to the low concentrations used, as it has been shown for T cells [73]; yet, it is notable that the concentrations we used were optimized to be non-cytotoxic. Furthermore, CBD abolished THC reduction of TNF α secretion (Figure 1E). Some data suggest that CBD can indirectly modulate THC via CB receptors [74] or by being an allosteric modulator that alters the efficacy of orthostatic ligands [75,76]. Filippes et al. showed reduced S100B secretion from LPS-treated mice pretreated with CBD; this reduction could be due to a systemic response in which CBD does not directly interact with EGC, like in our model [71].

Upon consumption, THC is metabolized in the liver to 11-OH-THC and then to the inactive metabolite THC-COOH [77]. THC-COOH did not reduce inflammatory markers in murine macrophages (Figure 1F); yet, it reduced all reactive glycolysis markers in EGC (Figures 1G,H and S4D). In the plant trichomes, THC is stored in its acidic form THCA [78]; THCA is not psychoactive, and, upon heating (smoking or baking), it undergoes a decarboxylation reaction and is transformed to THC [27]. At 1–70 nM, THCA significantly increased TNF α secretion from J774A1 macrophages. At higher concentrations, 100 nm–1 μM , no significant inflammatory effect was observed when compared to positive LPS control; yet, no reduction of TNF α secretion was measured for any of the concentrations tested (Figure 2A). In EGCs, THCA reduced both S100B secretion and expression, as well as GFAP expression at all concentrations tested (Figures 2B,C and S4C).

This indicates that THCA can prevent induction of reactive gliosis in EGCs. *C. sativa* flower extract fraction, rich in THCA, reduced IL-8 secretion, a marker for IBD inflammation, from HCT116 colonocytes, and CaCO2 cells using GPR55 antagonists blocked the reduction in IL-8, indicating that THCA exerts its effect through this receptor [79].

THCV is a minor cannabinoid from *C. sativa* with evidence of medicinal properties in metabolism [80], nausea [81], obesity and insulin sensitivity [35], pain [52], and inflammation [82]. Low concentrations, 0.2–3 nM, of THCV elevated murine macrophage TNF α secretion, whereas higher concentrations were not different from LPS-treated cells (Figure 4B). Overall, the results show that THCV did not improve inflammation markers in our system. This is in accordance with results of Rao et al. [82] that showed that THCV did not reduce LPS-induced NO production in RAW264.7 and similarly to the observed for keratinocytes [83].

CBC is considered one of the main four cannabinoids in the *Cannabis sativa* plant. It has been shown to have therapeutic properties through activation of TRPA1 and inhibition of degradation of cannabinoids [84–86]. An increase in TNF α secretion was generally observed in J774A1 macrophages. The lowest and the highest concentrations of CBC generally increased TNF α secretion; the most significant effect was achieved with 1 nM and 10–20 μ M compared to LPS control (Figure 2D). Concentrations of 10 nM to 1 μ M significantly reduced S100B secretion and expression in EGC (Figure 2E and Figure S4F respectively). However, GFAP mRNA expression was not changed by pretreatment with CBC. Cumulatively, these results show that CBC does not reduce inflammation on the tested primed cells according to the results of all of the markers that we measured (Figure 2F).

CBG may exert therapeutic effects through modulation of transient receptor potential (TRP) channels, cyclooxygenase (COX-1 and COX-2) enzymes, and cannabinoid 5-HT1A and α 2 adrenergic receptors [84,87–89]. Non-cytotoxic concentrations of CBG (0.05–20 μ M) did not reduce TNF α secretion (Figure 2G). At 1–10 μ M, CBG reduced S100B secretion by EGC, whereas, at 20 μ M, S100B secretion was elevated with and without LPS (Figure 2H). Expression levels of S100B were reduced in all tested concentrations (Figure S4E). Expression of GFAP was only reduced at 1 μ M CBG and was significantly increased at 20 μ M with or without LPS (Figure 2I). Collectively, it can be stated that CBG is effective on EGC at concentrations of 1–10 μ M.

To evaluate a more systematic cellular response, transcriptomic analysis was conducted on control untreated EGCs compared to EGCs treated with LPS 1 μ g/L for 24 h, pretreated for 1 h with 0.1 μ g/mL THC or 10 nM THC-COOH, and then with 1 μ g/L LPS (see Materials and Methods). Incubation with LPS-induced 23 DEGs (fold change > 1.6, p v < 0.05) (Figure 4A). Pathway analysis revealed that the main pathways affected by LPS were oxidative phosphorylation, mitochondrial dysfunction, and EIF2 signaling (Figure 5A). Oxidative phosphorylation and mitochondrial dysfunction were affected by downregulation of *cox6c*, *cox7b*, and *mt-co-1*, which are all part of the mitochondrial respiratory complex. It has been shown that the mitochondria are active in infection and inflammation through the release of cytokines and the activation of the inflammasomes [90]. Both *cox6c* and *cox7b* are part of Cytochrome c Oxidase, the terminal enzyme of the mitochondrial respiratory chain. The reduction in oxidative phosphorylation agrees with previous reports showing a shift from oxidative phosphorylation to glycolysis in LPS-induced glial cells [91,92]. Elf2 was shown to be activated via phosphorylation in RAW 264.7 cells by *Yersinia pseudotubercu* infection [93], causing a reduction of protein synthesis by negatively affecting the exchange of GDP to GTP in the β -subunit of eLF2. In BV-2 microglial cells, LPS can cause excessive mitochondrial fission and ROS generation [94]. LPS has been shown to elevate oxidative stress in BV-2 microglial cells and in the brain, as well as in other organs [95,96]. EIF2 phosphorylation is increased in murine macrophages that are exposed to bacterial infection, causing a reduction in protein synthesis [93]. IPA analysis identifies genetic networks that are affected by the DEG regardless of the direction of the expression change. Treatment with LPS affected developmental disorder, hereditary disorder, and metabolic disease

networks (12 DEG), along with cell cycle, cell death and survival, organismal injury, and abnormalities (11 DEG) (Figure 5D). This is in accordance with Juknat et al. [97].

Pretreatment for 1 h with 0.1 µg/mL THC before incubation with LPS resulted in 26 DEGs (10 upregulated and 16 downregulated) compared to no pre-incubation. The main pathways affected were mTOR signaling, EIF2, and retinoic acid receptor (RAR) activation, which was downregulated (z Score −2). mTOR was affected by downregulation of *ddit4*, *gm15483*, *mt-rnr1*, and *rps6kc1*. mTOR signaling has been implicated in inflammation processes. Mammalian target of rapamycin (mTor) is a conserved serine/threonine protein kinase belonging to the phosphoinositide 3-kinase (PI3K) family. It has been shown in CNS microglial cells that LPS activates mTor activity resulting in nitric oxide (NO) and prostaglandin E2 and D2 [98]. Inhibition of mTor using rapamycin inhibited these effects through reduction of COX2 and NOS2 [99]. RAR is essential for enteric nervous system (ENS) development. Knockout of RAR led to reduction of submucosal neurons yet did not reduce enteric glia cells primed by SOX10 [100]. Retinoic acid ameliorates IBD through NFκB signaling in the colitis model, along with RAW264.7 macrophages [101]. Most studies indicate activation of RAR in inflammation [100,101] yet our data indicate a reduction of the RAR pathway in glial cells pretreated with THC. Network analysis revealed that THC influenced the proteasome network (17 DEGs). It has been previously shown that mTOR regulates protein synthesis and degradation [102]. This is performed through control of the proteasome in nerve cells [103]. IPA analysis shows influences on both the mTOR signaling pathway and the proteasome network through pretreatment of THC.

The final metabolite of THC metabolism is THC-COOH. Pretreatment with this drug reduced S100B secretion and expression, as well as GFAP expression (Figure 1F,G). The pathway that was most affected by THC-COOH was IL6 signaling. IL6 is known to be elevated in activated EGCs [104]. Our data show downregulation of TGF-beta activated kinase 1 (*map3k7*) binding protein 1 (TAB1) and upregulation of TNF alpha induced protein 6 (*tnfaip6*) (−logFC −2.2 and 2, respectively). TAB1 is involved in IL6 activation through activation of IL-1 and NFκB signaling [105]. Activation of TNFAIP6 inhibits IL-6 secretion in lung cells [106]. Together, our results indicate that preincubation with THC-COOH could reduce IL-6 secretion by EGCs.

4. Materials and Methods

4.1. Cell Culture

4.1.1. J774A1 Murine Macrophages

J774A1 macrophages were purchased from the American type culture collection (ATCC, Manassas, VA, USA). Cells were cultured in 75 mm² flasks with Dulbecco's modified Eagle's medium (DMEM) (Sigma-Aldrich, Saint Louis, MO, USA) supplemented with 10% fetal bovine serum (Biological industries, Kibbutz Beit-Haemek, Israel), 1% penicillin–streptomycin (Biological industries), and 2.5 mL sodium pyruvate (Biological industries) until they reached 70% confluency at 37 °C under 5% CO₂.

4.1.2. Enteric Glial Cells

Enteric glial cell lines (EGC/PK060399egfr) were purchased from the American type culture collection (ATCC). Cells were thawed and grown in 75 mm² flasks to 70% confluence in DMEM medium containing 10% (Sigma-Aldrich) fetal bovine serum (FBS) (Biological industries) and 0.5% penicillin–streptomycin (Biological industries) at 37 °C under 5% CO₂. Cells were trypsinized (using 0.25%) (Invitrogen, Carlsbad, CA, USA) and transferred every 2–3 days.

4.2. Chemicals

Pure THC was purchased from BOL pharma (Revadim, Israel). Purified CBD was obtained from Tikun Olam Ltd. (Tel Aviv-Yafo, Israel). Sparstolonin B (*Ssnb*) was purchased from Sigma-Aldrich. LPS THCA, THCV CBC, CBG, CBA, and THC-COOH were purchased at HPLC standard grade (Restek, Bellefonte, PA, USA). All purified or synthetic

phytocannabinoids were dissolved in ethanol and later diluted with DMEM before addition to cells.

4.3. MTT 3-(4,5-Dimethylthiazol-2-yl)-2,5-diphenyltetrazolium Bromide

Cells were plated on 96-well plates at a concentration of 5×10^4 /0.2 mL/well and left to adhere for 2 h. The medium (DMEM D5796 Sigma-Aldrich) was replaced with media supplemented with different concentrations of test treatment. Cells were left in an incubator for 24 h (37 °C 5%CO₂). The medium was replaced with 180 µL of clear medium (DMEM 01-053-1A Biological industries) supplemented with 20 µL solubilized MTT with a final concentration of 0.5 mg/mL (Sigma Aldrich) for 2 h. After removal of MTT, 100 µL of dimethyl-sulfoxide (DMSO) was added and left on an orbital shaker for 20 min. Absorbance was measured in a spectrophotometer (Synergy H1, Agilent, CA, USA) at 550 nm.

4.4. In Vitro Treatments

The cells were plated at a concentration of $\sim 1 \times 10^6$ cells/mL and were pretreated with different concentrations of single phytocannabinoids and/or a mixture of phytocannabinoids for 1 h based on previous studies [107], after which LPS (*E. coli* 0111:B4, Sigma USA) was added for an additional 24 h. After treatment, the medium was removed for ELISA analysis (see below), and RNA/proteins were extracted from the respective cells.

4.5. Enzyme-Linked Immunosorbent Assay (ELISA)

The cell's growth medium was assayed for TNF α using ELISA, according to the manufacturer's instructions (Peprotech, Cranbury, NJ, USA), or for S100B, using a Simple-Step ELISA kit according to the manufacturer's instructions (Abcam, Waltham, MA, USA).

4.6. RNA Extraction and cDNA Synthesis

RNA was extracted using TRI reagent (Sigma GmbH, Mannheim, Germany) in combination with a PureLink column-based kit (Thermo Fisher, Waltham, MA, USA). RNA was quantified using Nanodrop 2000 (Thermo Fisher, Waltham, MA, USA). A total of 1.5 µg of RNA was used for synthesis of cDNA, using a qScript cDNA Synthesis Kit (Quanta Bio, Beverly, MA, USA).

4.7. Quantitative Reverse Transcription PCR (RT-qPCR)

Real time qPCR was preformed using fast SYBR green master mix (Applied Biosystems, Foster City, CA, USA) on a Quant studio 1 machine (Applied Biosystems). For normalization of gene expression in all reactions, we used the PPIA gene for TNF α gene normalization, and the GAPDH gene for S100B and GFAP genes normalization. Expression was quantified using the in-run standard curve method. Primers for relative gene expression are depicted in Supplemental Table S1.

4.8. RNA Sequencing Protocol and Computational Pipeline

For library construction and sequencing, total RNA was extracted, as described above. RNA-seq analysis was executed by the Crown Genomics institute of the Nancy and Stephen Grand Israel National Center for Personalized Medicine, Weizmann Institute of Science. A bulk adaptation of the MARS-Seq protocol [108,109] was used to generate RNA-Seq libraries for expression profiling. For sequence data analysis, assembly and annotation were performed, as described previously [110,111]. Differential analysis was performed using the DESeq2 package (1.26.0) [112] with the betaPrior, cooks cutoff, and independent filtering parameters set to False. Raw *p* values were adjusted for multiple testing using the procedure of Benjamini and Hochberg. Pipeline was run using snakemake [113]. DEGs were determined by a *p*-adj of <0.05, absolute fold changes > 1.6, and max raw counts > 10. For bioinformatics analysis, PCA, Hierarchical clustering, and K-Means clustering were performed. Standardized, log₂ normalized counts were used for the clustering analysis.

Clustering analysis was performed with R version 3.6.1. Data were submitted to GEO [114] accession GSE240225. DEGs, heatmaps, canonical pathways, and graphical networks were analyzed using Ingenuity Pathways Analysis (Ingenuity® Systems version 90348151, www.ingenuity.com).

4.9. Statistics

All statistics were performed with JMP pro 14 (SAS institute Inc., ver 11, Cary, NC, USA, 1989–2019) or GraphPad prism (version 8 GraphPad Software, San Diego, CA, USA, www.graphpad.com). Unless otherwise stated, data are expressed as mean \pm SE. Comparison between means of more than two groups were analyzed using means ANOVA and Tukey HSD.

5. Conclusions

Our results show that, while four different cannabinoids (CBC, CBG, THCA, and THC-COOH) reduced inflammation markers in EGCs, between all nine selected pure phytocannabinoids tested, only THC at low concentrations demonstrated significant reduction in TNF α secretion in J774A1 murine macrophages and EGC. This is in accordance with the known biphasic effect of THC, and it points to the advantage of using low doses of THC. Additionally, pretreatment of EGCs with low concentrations of THC markedly reduced S100B secretion and expression as well as GFAP expression. Taken together, these results show a significant immunosuppressive effect exerted by low doses of THC in our in vitro model. RNA-seq analyses and Ingenuity Pathways Analysis show that THC treatment affected the mTOR and RAR signaling pathway, while THC-COOH mainly affected the IL6 signaling pathway. The strength of the present study is that the putative anti-inflammatory effects of nine pure cannabinoids were analyzed in macrophages and enteric glial cells triggered to undergo inflammation in vitro with LPS tests that allowed us to select the most effective cannabinoid. The weakness of the present study is that we did not reflect these effects in in vivo studies, in which we hope to find similar effects in near future.

Supplementary Materials: The supporting information can be downloaded at: <https://www.mdpi.com/article/10.3390/ijms241914628/s1>.

Author Contributions: Conceptualization, B.S. and O.G.; methodology, G.C. and O.G.; software, O.G.; validation, G.C., O.G. and B.S.; formal analysis, G.C., O.G. and B.S.; investigation, G.C., O.G. and B.S.; resources, B.S.; data curation, G.C. and O.G.; writing—original draft preparation, G.C. and O.G.; writing—review and editing, B.S. and O.G.; supervision, B.S.; project administration, B.S. and O.G.; funding acquisition, B.S. All authors have read and agreed to the published version of the manuscript.

Funding: This research was funded by the Israeli Ministry of Agriculture grant number 12-05-0035.

Institutional Review Board Statement: Not applicable.

Informed Consent Statement: Not applicable.

Data Availability Statement: Sequencing data is available at: <https://www.ncbi.nlm.nih.gov/geo/query/acc.cgi?acc=GSE240225>.

Acknowledgments: We like to that Alona Volov for graphical editing of the figures.

Conflicts of Interest: The authors declare no conflict of interest.

References

1. Baghdadi, M.B.; Kim, T.-H. The multiple roles of enteric glial cells in intestinal homeostasis and regeneration. *Semin. Cell Dev. Biol.* **2023**, *150–151*, 43–49. [[CrossRef](#)]
2. Bain, C.C.; Scott, C.L.; Uronen-Hansson, H.; Gudjonsson, S.; Jansson, O.; Grip, O.; Williams, M.; Malissen, B.; Agace, W.W.; Mowat, A.M. Resident and pro-inflammatory macrophages in the colon represent alternative context-dependent fates of the same Ly6Chi monocyte precursors. *Mucosal Immunol.* **2013**, *6*, 498–510. [[CrossRef](#)]
3. Heinsbroek, S.E.; Gordon, S. The role of macrophages in inflammatory bowel diseases. *Expert Rev. Mol. Med.* **2009**, *11*, e14. [[CrossRef](#)]

4. Mahida, Y.R.; Patel, S.; Gionchetti, P.; Vaux, D.; Jewell, D.P. Macrophage subpopulations in lamina propria of normal and inflamed colon and terminal ileum. *Gut* **1989**, *30*, 826–834. [[CrossRef](#)]
5. Gordon, S.; Martinez, F.O. Alternative activation of macrophages: Mechanism and functions. *Immunity* **2010**, *32*, 593–604. [[CrossRef](#)]
6. Qiao, K.; Le Page, L.M.; Chaumeil, M.M. Non-Invasive Differentiation of M1 and M2 Activation in Macrophages Using Hyperpolarized ¹³C MRS of Pyruvate and DHA at 1.47 Tesla. *Metabolites* **2021**, *11*, 410. [[CrossRef](#)]
7. Mantovani, A.; Sica, A.; Sozzani, S.; Allavena, P.; Vecchi, A.; Locati, M. The chemokine system in diverse forms of macrophage activation and polarization. *Trends Immunol.* **2004**, *25*, 677–686. [[CrossRef](#)] [[PubMed](#)]
8. Brown, B.N.; Valentin, J.E.; Stewart-Akers, A.M.; McCabe, G.P.; Badylak, S.F. Macrophage phenotype and remodeling outcomes in response to biologic scaffolds with and without a cellular component. *Biomaterials* **2009**, *30*, 1482–1491. [[CrossRef](#)] [[PubMed](#)]
9. Shi, C.; Pamer, E.G. Monocyte recruitment during infection and inflammation. *Nat. Rev. Immunol.* **2011**, *11*, 762–774. [[CrossRef](#)] [[PubMed](#)]
10. Michetti, F.; Di Sante, G.; Clementi, M.E.; Sampaiolese, B.; Casalbore, P.; Volonte, C.; Romano Spica, V.; Parnigotto, P.P.; Di Liddo, R.; Amadio, S.; et al. Growing role of S100B protein as a putative therapeutic target for neurological- and nonneurological-disorders. *Neurosci. Biobehav. Rev.* **2021**, *127*, 446–458. [[CrossRef](#)]
11. Fuss, I.J.; Neurath, M.; Boirivant, M.; Klein, J.S.; de la Motte, C.; Strong, S.A.; Fiocchi, C.; Strober, W. Disparate CD4+ lamina propria (LP) lymphokine secretion profiles in inflammatory bowel disease. Crohn's disease LP cells manifest increased secretion of IFN-gamma, whereas ulcerative colitis LP cells manifest increased secretion of IL-5. *J. Immunol.* **1996**, *157*, 1261–1270. [[CrossRef](#)]
12. Xu, X.R.; Liu, C.Q.; Feng, B.S.; Liu, Z.J. Dysregulation of mucosal immune response in pathogenesis of inflammatory bowel disease. *World J. Gastroenterol.* **2014**, *20*, 3255–3264. [[CrossRef](#)] [[PubMed](#)]
13. Yen, D.; Cheung, J.; Scheerens, H.; Poulet, F.; McClanahan, T.; McKenzie, B.; Kleinschek, M.A.; Owyang, A.; Mattson, J.; Blumenschein, W.; et al. IL-23 is essential for T cell-mediated colitis and promotes inflammation via IL-17 and IL-6. *J. Clin. Investig.* **2006**, *116*, 1310–1316. [[CrossRef](#)]
14. Dvorak, A.M.; Onderdonk, A.B.; McLeod, R.S.; Monahan-Earley, R.A.; Cullen, J.; Antonioli, D.A.; Blair, J.E.; Morgan, E.S.; Cisneros, R.L.; Estrella, P.; et al. Axonal necrosis of enteric autonomic nerves in continent ileal pouches. Possible implications for pathogenesis of Crohn's disease. *Ann. Surg.* **1993**, *217*, 260–271. [[CrossRef](#)]
15. Liu, C.; Yang, J. Enteric Glial Cells in Immunological Disorders of the Gut. *Front. Cell. Neurosci.* **2022**, *16*, 895871. [[CrossRef](#)] [[PubMed](#)]
16. Cirillo, C.; Sarnelli, G.; Esposito, G.; Grosso, M.; Petruzzelli, R.; Izzo, P.; Cali, G.; D'Armiento, F.P.; Rocco, A.; Nardone, G.; et al. Increased mucosal nitric oxide production in ulcerative colitis is mediated in part by the enteroglia-derived S100B protein. *Neurogastroenterol. Motil.* **2009**, *21*, 1209–e1112. [[CrossRef](#)] [[PubMed](#)]
17. Esposito, G.; Cirillo, C.; Sarnelli, G.; De Filippis, D.; D'Armiento, F.P.; Rocco, A.; Nardone, G.; Petruzzelli, R.; Grosso, M.; Izzo, P.; et al. Enteric glial-derived S100B protein stimulates nitric oxide production in celiac disease. *Gastroenterology* **2007**, *133*, 918–925. [[CrossRef](#)]
18. Progatky, F.; Pachnis, V. The role of enteric glia in intestinal immunity. *Curr. Opin. Immunol.* **2022**, *77*, 102183. [[CrossRef](#)]
19. Abdo, H.; Derkinderen, P.; Gomes, P.; Chevalier, J.; Aubert, P.; Masson, D.; Galmiche, J.P.; Vanden Berghe, P.; Neunlist, M.; Lardeux, B. Enteric glial cells protect neurons from oxidative stress in part via reduced glutathione. *FASEB J.* **2010**, *24*, 1082–1094. [[CrossRef](#)]
20. Jessen, K.R.; Mirsky, R. Astrocyte-like glia in the peripheral nervous system: An immunohistochemical study of enteric glia. *J. Neurosci.* **1983**, *3*, 2206–2218. [[CrossRef](#)]
21. Cabarrocas, J.; Savidge, T.C.; Liblau, R.S. Role of enteric glial cells in inflammatory bowel disease. *Glia* **2003**, *41*, 81–93. [[CrossRef](#)] [[PubMed](#)]
22. Capoccia, E.; Cirillo, C.; Gigli, S.; Pesce, M.; D'Alessandro, A.; Cuomo, R.; Sarnelli, G.; Steardo, L.; Esposito, G. Enteric glia: A new player in inflammatory bowel diseases. *Int. J. Immunopathol. Pharmacol.* **2015**, *28*, 443–451. [[CrossRef](#)]
23. da Cunha Franceschi, R.; Nardin, P.; Machado, C.V.; Tortorelli, L.S.; Martinez-Pereira, M.A.; Zanutto, C.; Gonçalves, C.A.; Zancan, D.M. Enteric glial reactivity to systemic LPS administration: Changes in GFAP and S100B protein. *Neurosci. Res.* **2017**, *119*, 15–23. [[CrossRef](#)] [[PubMed](#)]
24. Barbara, G.; Wang, B.; Stanghellini, V.; de Giorgio, R.; Cremon, C.; Di Nardo, G.; Trevisani, M.; Campi, B.; Geppetti, P.; Tonini, M.; et al. Mast cell-dependent excitation of visceral-nociceptive sensory neurons in irritable bowel syndrome. *Gastroenterology* **2007**, *132*, 26–37. [[CrossRef](#)] [[PubMed](#)]
25. Grundmann, D.; Loris, E.; Maas-Omlor, S.; Huang, W.; Scheller, A.; Kirchoff, F.; Schäfer, K.-H. Enteric Glia: S100, GFAP, and Beyond. *Anat. Rec.* **2019**, *302*, 1333–1344. [[CrossRef](#)]
26. Lu, H.C.; Mackie, K. Review of the Endocannabinoid System. *Biol. Psychiatry Cogn. Neurosci. Neuroimaging* **2021**, *6*, 607–615. [[CrossRef](#)]
27. Grotenhermen, F. Pharmacokinetics and pharmacodynamics of cannabinoids. *Clin. Pharmacokinet.* **2003**, *42*, 327–360. [[CrossRef](#)]
28. Morales, P.; Hurst, D.P.; Reggio, P.H. Molecular Targets of the Phytocannabinoids: A Complex Picture. *Prog. Chem. Org. Nat. Prod.* **2017**, *103*, 103–131. [[CrossRef](#)]
29. Sharkey, K.A.; Wiley, J.W. The Role of the Endocannabinoid System in the Brain-Gut Axis. *Gastroenterology* **2016**, *151*, 252–266. [[CrossRef](#)]

30. Bhat, N.R.; Zhang, P.; Hogan, E.L. Thrombin activates mitogen-activated protein kinase in primary astrocyte cultures. *J. Cell Physiol.* **1995**, *165*, 417–424. [[CrossRef](#)]
31. Zou, S.; Kumar, U. Cannabinoid Receptors and the Endocannabinoid System: Signaling and Function in the Central Nervous System. *Int. J. Mol. Sci.* **2018**, *19*, 833. [[CrossRef](#)]
32. Navarrete, M.; Araque, A. Endocannabinoids mediate neuron-astrocyte communication. *Neuron* **2008**, *57*, 883–893. [[CrossRef](#)]
33. Alhouayek, M.; Muccioli, G.G. The endocannabinoid system in inflammatory bowel diseases: From pathophysiology to therapeutic opportunity. *Trends Mol. Med.* **2012**, *18*, 615–625. [[CrossRef](#)]
34. Pertwee, R.G. Pharmacology of cannabinoid CB1 and CB2 receptors. *Pharmacol. Ther.* **1997**, *74*, 129–180. [[CrossRef](#)]
35. McPartland, J.M.; Duncan, M.; Di Marzo, V.; Pertwee, R.G. Are cannabidiol and Δ^9 -tetrahydrocannabivarin negative modulators of the endocannabinoid system? A systematic review. *Br. J. Pharmacol.* **2015**, *172*, 737–753. [[CrossRef](#)]
36. Trautmann, S.M.; Sharkey, K.A. The Endocannabinoid System and Its Role in Regulating the Intrinsic Neural Circuitry of the Gastrointestinal Tract. *Int. Rev. Neurobiol.* **2015**, *125*, 85–126. [[CrossRef](#)]
37. Wright, K.; Rooney, N.; Feeney, M.; Tate, J.; Robertson, D.; Welham, M.; Ward, S. Differential expression of cannabinoid receptors in the human colon: Cannabinoids promote epithelial wound healing. *Gastroenterology* **2005**, *129*, 437–453. [[CrossRef](#)] [[PubMed](#)]
38. Galiegue, S.; Mary, S.; Marchand, J.; Dussossoy, D.; Carriere, D.; Carayon, P.; Bouaboula, M.; Shire, D.; Le Fur, G.; Casellas, P. Expression of central and peripheral cannabinoid receptors in human immune tissues and leukocyte subpopulations. *Eur. J. Biochem.* **1995**, *232*, 54–61. [[CrossRef](#)] [[PubMed](#)]
39. Spiller, K.J.; Bi, G.H.; He, Y.; Galaj, E.; Gardner, E.L.; Xi, Z.X. Cannabinoid CB(1) and CB(2) receptor mechanisms underlie cannabis reward and aversion in rats. *Br. J. Pharmacol.* **2019**, *176*, 1268–1281. [[CrossRef](#)]
40. Galiazzo, G.; Giancola, F.; Stanzani, A.; Fracassi, F.; Bernardini, C.; Forni, M.; Pietra, M.; Chiocchetti, R. Localization of cannabinoid receptors CB1, CB2, GPR55, and PPAR α in the canine gastrointestinal tract. *Histochem. Cell Biol.* **2018**, *150*, 187–205. [[CrossRef](#)] [[PubMed](#)]
41. Izzo, A.A.; Fezza, F.; Capasso, R.; Bisogno, T.; Pinto, L.; Iuvone, T.; Esposito, G.; Mascolo, N.; Di Marzo, V.; Capasso, F. Cannabinoid CB1-receptor mediated regulation of gastrointestinal motility in mice in a model of intestinal inflammation. *Br. J. Pharmacol.* **2001**, *134*, 563–570. [[CrossRef](#)] [[PubMed](#)]
42. Duncan, M.; Mouihate, A.; Mackie, K.; Keenan, C.M.; Buckley, N.E.; Davison, J.S.; Patel, K.D.; Pittman, Q.J.; Sharkey, K.A. Cannabinoid CB2 receptors in the enteric nervous system modulate gastrointestinal contractility in lipopolysaccharide-treated rats. *Am. J. Physiol. Gastrointest. Liver Physiol.* **2008**, *295*, G78–G87. [[CrossRef](#)]
43. Liang, Q.; Dong, S.; Lei, L.; Liu, J.; Zhang, J.; Li, J.; Duan, J.; Fan, D. Protective effects of Sparstolonin B, a selective TLR2 and TLR4 antagonist, on mouse endotoxin shock. *Cytokine* **2015**, *75*, 302–309. [[CrossRef](#)]
44. Dattaroy, D.; Seth, R.K.; Das, S.; Alhasson, F.; Chandrashekar, V.; Michelotti, G.; Fan, D.; Nagarkatti, M.; Nagarkatti, P.; Diehl, A.M.; et al. Sparstolonin B attenuates early liver inflammation in experimental NASH by modulating TLR4 trafficking in lipid rafts via NADPH oxidase activation. *Am. J. Physiol. Gastrointest. Liver Physiol.* **2016**, *310*, G510–G525. [[CrossRef](#)]
45. Cornet, A.; Savidge, T.C.; Cabarrocas, J.; Deng, W.L.; Colombel, J.F.; Lassmann, H.; Desreumaux, P.; Liblau, R.S. Enterocolitis induced by autoimmune targeting of enteric glial cells: A possible mechanism in Crohn's disease? *Proc. Natl. Acad. Sci. USA* **2001**, *98*, 13306–13311. [[CrossRef](#)]
46. Kumar, P.; Nagarajan, A.; Uchil, P.D. Analysis of Cell Viability by the MTT Assay. *Cold Spring Harb. Protoc.* **2018**, *2018*. [[CrossRef](#)]
47. Dos Santos, R.G.; Guimaraes, F.S.; Crippa, J.A.S.; Hallak, J.E.C.; Rossi, G.N.; Rocha, J.M.; Zuardi, A.W. Serious adverse effects of cannabidiol (CBD): A review of randomized controlled trials. *Expert Opin. Drug. Metab. Toxicol.* **2020**, *16*, 517–526. [[CrossRef](#)]
48. Matsunaga, T.; Iwawaki, Y.; Watanabe, K.; Yamamoto, I.; Kageyama, T.; Yoshimura, H. Metabolism of Δ^9 -tetrahydrocannabinol by cytochrome P450 isozymes purified from hepatic microsomes of monkeys. *Life Sci.* **1995**, *56*, 2089–2095. [[CrossRef](#)] [[PubMed](#)]
49. Burstein, S.H. The cannabinoid acids: Nonpsychoactive derivatives with therapeutic potential. *Pharmacol. Ther.* **1999**, *82*, 87–96. [[CrossRef](#)] [[PubMed](#)]
50. Happyana, N.; Agnolet, S.; Muntendam, R.; Van Dam, A.; Schneider, B.; Kayser, O. Analysis of cannabinoids in laser-microdissected trichomes of medicinal Cannabis sativa using LCMS and cryogenic NMR. *Phytochemistry* **2013**, *87*, 51–59. [[CrossRef](#)] [[PubMed](#)]
51. Dewey, W.L. Cannabinoid pharmacology. *Pharmacol. Rev.* **1986**, *38*, 151–178. [[CrossRef](#)]
52. Bolognini, D.; Costa, B.; Maione, S.; Comelli, F.; Marini, P.; Di Marzo, V.; Parolaro, D.; Ross, R.A.; Gauson, L.A.; Cascio, M.G.; et al. The plant cannabinoid Delta9-tetrahydrocannabivarin can decrease signs of inflammation and inflammatory pain in mice. *Br. J. Pharmacol.* **2010**, *160*, 677–687. [[CrossRef](#)] [[PubMed](#)]
53. Bae, J.S.; Jeon, Y.; Kim, S.M.; Jang, J.Y.; Park, M.K.; Kim, I.-H.; Hwang, D.S.; Lim, D.-S.; Lee, H. Depletion of MOB1A/B causes intestinal epithelial degeneration by suppressing Wnt activity and activating BMP/TGF- β signaling. *Cell Death Dis.* **2018**, *9*, 1083. [[CrossRef](#)]
54. Li, F.J.; Zheng, S.R.; Wang, D.M. Adrenomedullin: An important participant in neurological diseases. *Neural Regen. Res.* **2020**, *15*, 1199–1207. [[CrossRef](#)]
55. Mahil, S.K.; Twelves, S.; Farkas, K.; Setta-Kaffetzi, N.; Burden, A.D.; Gach, J.E.; Irvine, A.D.; Képiró, L.; Mockenhaupt, M.; Oon, H.H.; et al. AP1S3 Mutations Cause Skin Autoinflammation by Disrupting Keratinocyte Autophagy and Up-Regulating IL-36 Production. *J. Investig. Dermatol.* **2016**, *136*, 2251–2259. [[CrossRef](#)] [[PubMed](#)]

56. Chwee, J.Y.; Khatoo, M.; Tan, N.Y.; Gasser, S. Apoptotic Cells Release IL1 Receptor Antagonist in Response to Genotoxic Stress. *Cancer Immunol. Res.* **2016**, *4*, 294–302. [[CrossRef](#)]
57. Leon, G.; Hussey, S.; Walsh, P.T. The Diverse Roles of the IL-36 Family in Gastrointestinal Inflammation and Resolution. *Inflamm. Bowel Dis.* **2021**, *27*, 440–450. [[CrossRef](#)] [[PubMed](#)]
58. Rashid, M.-u.; Lorzadeh, S.; Gao, A.; Ghavami, S.; Coombs, K.M. PSMA2 knockdown impacts expression of proteins involved in immune and cellular stress responses in human lung cells. *Biochim. Biophys. Acta (BBA)-Mol. Basis Dis.* **2023**, *1869*, 166617. [[CrossRef](#)]
59. Zhang, J.; Zhao, Y.; Hou, T.; Zeng, H.; Kalambhe, D.; Wang, B.; Shen, X.; Huang, Y. Macrophage-based nanotherapeutic strategies in ulcerative colitis. *J. Control. Release* **2020**, *320*, 363–380. [[CrossRef](#)]
60. Sharkey, K.A. Emerging roles for enteric glia in gastrointestinal disorders. *J. Clin. Investig.* **2015**, *125*, 918–925. [[CrossRef](#)]
61. Neunlist, M.; Rolli-Derkinderen, M.; Latorre, R.; Van Landeghem, L.; Coron, E.; Derkinderen, P.; De Giorgio, R. Enteric glial cells: Recent developments and future directions. *Gastroenterology* **2014**, *147*, 1230–1237. [[CrossRef](#)]
62. López-Gómez, L.; Szymaszkiwicz, A.; Zielińska, M.; Abalo, R. The Enteric Glia and Its Modulation by the Endocannabinoid System, a New Target for Cannabinoid-Based Nutraceuticals? *Molecules* **2022**, *27*, 6773. [[CrossRef](#)] [[PubMed](#)]
63. Pertwee, R.G. The diverse CB₁ and CB₂ receptor pharmacology of three plant cannabinoids: Δ^9 -tetrahydrocannabinol, cannabidiol and Δ^9 -tetrahydrocannabivarin. *Br. J. Pharmacol.* **2008**, *153*, 199–215. [[CrossRef](#)] [[PubMed](#)]
64. Margulies, J.E.; Hammer, R.P. Δ^9 -Tetrahydrocannabinol alters cerebral metabolism in a biphasic, dose-dependent manner in rat brain. *Eur. J. Pharmacol.* **1991**, *202*, 373–378. [[CrossRef](#)] [[PubMed](#)]
65. Becker, W.; Alrafas, H.R.; Busbee, P.B.; Walla, M.D.; Wilson, K.; Miranda, K.; Cai, G.; Putluri, V.; Putluri, N.; Nagarkatti, M.; et al. Cannabinoid Receptor Activation on Haematopoietic Cells and Enterocytes Protects against Colitis. *J. Crohn's Colitis* **2020**, *15*, 1032–1048. [[CrossRef](#)] [[PubMed](#)]
66. Yekhtin, Z.; Khuja, I.; Meiri, D.; Or, R.; Almogi-Hazan, O. Differential Effects of Δ^9 Tetrahydrocannabinol (THC)- and Cannabidiol (CBD)-Based Cannabinoid Treatments on Macrophage Immune Function In Vitro and on Gastrointestinal Inflammation in a Murine Model. *Biomedicines* **2022**, *10*, 1793. [[CrossRef](#)]
67. Sarne, Y.; Toledano, R.; Rachmany, L.; Sasson, E.; Doron, R. Reversal of age-related cognitive impairments in mice by an extremely low dose of tetrahydrocannabinol. *Neurobiol. Aging* **2018**, *61*, 177–186. [[CrossRef](#)]
68. Bilkei-Gorzo, A.; Albayram, O.; Draffehn, A.; Michel, K.; Piyanova, A.; Oppenheimer, H.; Dvir-Ginzberg, M.; Racz, I.; Ulas, T.; Imbeault, S.; et al. A chronic low dose of Delta(9)-tetrahydrocannabinol (THC) restores cognitive function in old mice. *Nat. Med.* **2017**, *23*, 782–787. [[CrossRef](#)]
69. MacKenzie, S.; Fernandez-Troy, N.; Espel, E. Post-transcriptional regulation of TNF-alpha during in vitro differentiation of human monocytes/macrophages in primary culture. *J. Leukoc. Biol.* **2002**, *71*, 1026–1032. [[CrossRef](#)]
70. MacKenzie, S.; Planas, J.V.; Goetz, F.W. LPS-stimulated expression of a tumor necrosis factor-alpha mRNA in primary trout monocytes and in vitro differentiated macrophages. *Dev. Comp. Immunol.* **2003**, *27*, 393–400. [[CrossRef](#)]
71. De Filippis, D.; Esposito, G.; Cirillo, C.; Cipriano, M.; De Winter, B.Y.; Scuderi, C.; Sarnelli, G.; Cuomo, R.; Steardo, L.; De Man, J.G.; et al. Cannabidiol reduces intestinal inflammation through the control of neuroimmune axis. *PLoS ONE* **2011**, *6*, e28159. [[CrossRef](#)]
72. Di Marzo, V. New approaches and challenges to targeting the endocannabinoid system. *Nat. Rev. Drug. Discov.* **2018**, *17*, 623–639. [[CrossRef](#)]
73. Chen, W.; Kaplan, B.L.; Pike, S.T.; Topper, L.A.; Lichorobiec, N.R.; Simmons, S.O.; Ramabhadran, R.; Kaminski, N.E. Magnitude of stimulation dictates the cannabinoid-mediated differential T cell response to HIVgp120. *J. Leukoc. Biol.* **2012**, *92*, 1093–1102. [[CrossRef](#)]
74. Zuardi, A.W.; Shirakawa, I.; Finkelfarb, E.; Karniol, I.G. Action of cannabidiol on the anxiety and other effects produced by delta 9-THC in normal subjects. *Psychopharmacology* **1982**, *76*, 245–250. [[CrossRef](#)]
75. Hayakawa, K.; Mishima, K.; Hazekawa, M.; Sano, K.; Irie, K.; Orito, K.; Egawa, T.; Kitamura, Y.; Uchida, N.; Nishimura, R.; et al. Cannabidiol potentiates pharmacological effects of Delta(9)-tetrahydrocannabinol via CB(1) receptor-dependent mechanism. *Brain Res.* **2008**, *1188*, 157–164. [[CrossRef](#)]
76. Laprairie, R.B.; Bagher, A.M.; Kelly, M.E.; Denovan-Wright, E.M. Cannabidiol is a negative allosteric modulator of the cannabinoid CB1 receptor. *Br. J. Pharmacol.* **2015**, *172*, 4790–4805. [[CrossRef](#)]
77. Watanabe, K.; Yamaori, S.; Funahashi, T.; Kimura, T.; Yamamoto, I. Cytochrome P450 enzymes involved in the metabolism of tetrahydrocannabinols and cannabinol by human hepatic microsomes. *Life Sci.* **2007**, *80*, 1415–1419. [[CrossRef](#)] [[PubMed](#)]
78. Verhoeckx, K.C.; Korthout, H.A.; van Meeteren-Kreikamp, A.P.; Ehlert, K.A.; Wang, M.; van der Greef, J.; Rodenburg, R.J.; Witkamp, R.F. Unheated Cannabis sativa extracts and its major compound THC-acid have potential immuno-modulating properties not mediated by CB1 and CB2 receptor coupled pathways. *Int. Immunopharmacol.* **2006**, *6*, 656–665. [[CrossRef](#)] [[PubMed](#)]
79. Rameshprabu, N.; Moran, M.; Aurel, I.; Gopinath, S.; Smadar, W.; Marcelo, F.; Ahmad, N.; Oded, S.; Puja, K.; Diana, N.; et al. Anti-Inflammatory Activity in Colon Models Is Derived from Δ^9 -Tetrahydrocannabinolic Acid That Interacts with Additional Compounds in Cannabis Extracts. *Cannabis Cannabinoid Res.* **2017**, *2*, 167–182. [[CrossRef](#)]
80. Silvestri, C.; Paris, D.; Martella, A.; Melck, D.; Guadagnino, I.; Cawthorne, M.; Motta, A.; Di Marzo, V. Two non-psychoactive cannabinoids reduce intracellular lipid levels and inhibit hepatosteatosis. *J. Hepatol.* **2015**, *62*, 1382–1390. [[CrossRef](#)]

81. Rock, E.M.; Sticht, M.A.; Duncan, M.; Stott, C.; Parker, L.A. Evaluation of the potential of the phytocannabinoids, cannabidivarin (CBDV) and Delta(9)-tetrahydrocannabivarin (THCV), to produce CB1 receptor inverse agonism symptoms of nausea in rats. *Br. J. Pharmacol.* **2013**, *170*, 671–678. [[CrossRef](#)]
82. Romano, B.; Pagano, E.; Orlando, P.; Capasso, R.; Cascio, M.G.; Pertwee, R.; Marzo, V.D.; Izzo, A.A.; Borrelli, F. Pure Δ^9 -tetrahydrocannabivarin and a Cannabis sativa extract with high content in Δ^9 -tetrahydrocannabivarin inhibit nitrite production in murine peritoneal macrophages. *Pharmacol. Res.* **2016**, *113*, 199–208. [[CrossRef](#)]
83. Tortolani, D.; Di Meo, C.; Standoli, S.; Ciaramellano, F.; Kadhim, S.; Hsu, E.; Rapino, C.; Maccarrone, M. Rare Phytocannabinoids Exert Anti-Inflammatory Effects on Human Keratinocytes via the Endocannabinoid System and MAPK Signaling Pathway. *Int. J. Mol. Sci.* **2023**, *24*, 2721. [[CrossRef](#)] [[PubMed](#)]
84. De Petrocellis, L.; Ligresti, A.; Moriello, A.S.; Allara, M.; Bisogno, T.; Petrosino, S.; Stott, C.G.; Di Marzo, V. Effects of cannabinoids and cannabinoid-enriched Cannabis extracts on TRP channels and endocannabinoid metabolic enzymes. *Br. J. Pharmacol.* **2011**, *163*, 1479–1494. [[CrossRef](#)]
85. Romano, B.; Borrelli, F.; Fasolino, I.; Capasso, R.; Piscitelli, F.; Cascio, M.; Pertwee, R.; Coppola, D.; Vassallo, L.; Orlando, P.; et al. The cannabinoid TRPA1 agonist cannabichromene inhibits nitric oxide production in macrophages and ameliorates murine colitis. *Br. J. Pharmacol.* **2013**, *169*, 213–229. [[CrossRef](#)] [[PubMed](#)]
86. Izzo, A.A.; Capasso, R.; Aviello, G.; Borrelli, F.; Romano, B.; Piscitelli, F.; Gallo, L.; Capasso, F.; Orlando, P.; Di Marzo, V. Inhibitory effect of cannabichromene, a major non-psychotropic cannabinoid extracted from Cannabis sativa, on inflammation-induced hypermotility in mice. *Br. J. Pharmacol.* **2012**, *166*, 1444–1460. [[CrossRef](#)] [[PubMed](#)]
87. Ligresti, A.; Moriello, A.S.; Starowicz, K.; Matias, I.; Pisanti, S.; De Petrocellis, L.; Laezza, C.; Portella, G.; Bifulco, M.; Di Marzo, V. Antitumor activity of plant cannabinoids with emphasis on the effect of cannabidiol on human breast carcinoma. *J. Pharmacol. Exp. Ther.* **2006**, *318*, 1375–1387. [[CrossRef](#)]
88. Ruhaak, L.R.; Felth, J.; Karlsson, P.C.; Rafter, J.J.; Verpoorte, R.; Bohlin, L. Evaluation of the cyclooxygenase inhibiting effects of six major cannabinoids isolated from Cannabis sativa. *Biol. Pharm. Bull.* **2011**, *34*, 774–778. [[CrossRef](#)] [[PubMed](#)]
89. Deininger, M.H.; Meyermann, R.; Trautmann, K.; Morgalla, M.; Duffner, F.; Grote, E.H.; Wickboldt, J.; Schluesener, H.J. Cyclooxygenase (COX)-1 expressing macrophages/microglial cells and COX-2 expressing astrocytes accumulate during oligodendrogloma progression. *Brain Res.* **2000**, *885*, 111–116. [[CrossRef](#)]
90. Andrieux, P.; Chevillard, C.; Cunha-Neto, E.; Nunes, J.P.S. Mitochondria as a Cellular Hub in Infection and Inflammation. *Int. J. Mol. Sci.* **2021**, *22*, 11338. [[CrossRef](#)] [[PubMed](#)]
91. Cheng, J.; Zhang, R.; Xu, Z.; Ke, Y.; Sun, R.; Yang, H.; Zhang, X.; Zhen, X.; Zheng, L.-T. Early glycolytic reprogramming controls microglial inflammatory activation. *J. Neuroinflamm.* **2021**, *18*, 129. [[CrossRef](#)]
92. Orihuela, R.; McPherson, C.A.; Harry, G.J. Microglial M1/M2 polarization and metabolic states. *Br. J. Pharmacol.* **2016**, *173*, 649–665. [[CrossRef](#)] [[PubMed](#)]
93. Shrestha, N.; Bahnan, W.; Wiley, D.J.; Barber, G.; Fields, K.A.; Schesser, K. Eukaryotic Initiation Factor 2 (eIF2) Signaling Regulates Proinflammatory Cytokine Expression and Bacterial Invasion. *J. Biol. Chem.* **2012**, *287*, 28738–28744. [[CrossRef](#)] [[PubMed](#)]
94. Lee, D.G.; Nam, B.R.; Huh, J.-W.; Lee, D.-S. Isoliquiritigenin Reduces LPS-Induced Inflammation by Preventing Mitochondrial Fission in BV-2 Microglial Cells. *Inflammation* **2021**, *44*, 714–724. [[CrossRef](#)] [[PubMed](#)]
95. Seemann, S.; Zohles, F.; Lupp, A. Comprehensive comparison of three different animal models for systemic inflammation. *J. Biomed. Sci.* **2017**, *24*, 60. [[CrossRef](#)]
96. Liu, J.; Zong, Z.; Zhang, W.; Chen, Y.; Wang, X.; Shen, J.; Yang, C.; Liu, X.; Deng, H. Nicotinamide Mononucleotide Alleviates LPS-Induced Inflammation and Oxidative Stress via Decreasing COX-2 Expression in Macrophages. *Front. Mol. Biosci.* **2021**, *8*, 702107. [[CrossRef](#)]
97. Juknat, A.; Pietr, M.; Kozela, E.; Rimmerman, N.; Levy, R.; Gao, F.; Coppola, G.; Geschwind, D.; Vogel, Z. Microarray and Pathway Analysis Reveal Distinct Mechanisms Underlying Cannabinoid-Mediated Modulation of LPS-Induced Activation of BV-2 Microglial Cells. *PLoS ONE* **2013**, *8*, e61462. [[CrossRef](#)]
98. Dello Russo, C.; Lisi, L.; Feinstein, D.L.; Navarra, P. mTOR kinase, a key player in the regulation of glial functions: Relevance for the therapy of multiple sclerosis. *Glia* **2013**, *61*, 301–311. [[CrossRef](#)]
99. Dello Russo, C.; Lisi, L.; Tringali, G.; Navarra, P. Involvement of mTOR kinase in cytokine-dependent microglial activation and cell proliferation. *Biochem. Pharmacol.* **2009**, *78*, 1242–1251. [[CrossRef](#)]
100. Gao, T.; Wright-Jin, E.C.; Sengupta, R.; Anderson, J.B.; Heuckeroth, R.O. Cell-autonomous retinoic acid receptor signaling has stage-specific effects on mouse enteric nervous system. *J. Clin. Insight.* **2021**, *6*, 145854. [[CrossRef](#)]
101. Hong, K.; Zhang, Y.; Guo, Y.; Xie, J.; Wang, J.; He, X.; Lu, N.; Bai, A. All-trans retinoic acid attenuates experimental colitis through inhibition of NF- κ B signaling. *Immunol. Lett.* **2014**, *162*, 34–40. [[CrossRef](#)]
102. Zhang, Y.; Nicholatos, J.; Dreier, J.R.; Ricoult, S.J.; Widenmaier, S.B.; Hotamisligil, G.S.; Kwiatkowski, D.J.; Manning, B.D. Coordinated regulation of protein synthesis and degradation by mTORC1. *Nature* **2014**, *513*, 440–443. [[CrossRef](#)] [[PubMed](#)]
103. Kouloulia, S.; Hallin, E.I.; Simbriger, K.; Amorim, I.S.; Lach, G.; Amvrosiadis, T.; Chalkiadaki, K.; Kampaite, A.; Truong, V.T.; Hooshmandi, M.; et al. Raptor-Mediated Proteasomal Degradation of Deamidated 4E-BP2 Regulates Postnatal Neuronal Translation and NF- κ B Activity. *Cell Rep.* **2019**, *29*, 3620–3635.e7. [[CrossRef](#)] [[PubMed](#)]
104. Rühl, A.; Franzke, S.; Collins, S.M.; Stremmel, W. Interleukin-6 expression and regulation in rat enteric glial cells. *Am. J. Physiol.-Gastrointest. Liver Physiol.* **2001**, *280*, G1163–G1171. [[CrossRef](#)] [[PubMed](#)]

105. Yu, Y.; Ge, N.; Xie, M.; Sun, W.; Burlingame, S.; Pass, A.K.; Nuchtern, J.G.; Zhang, D.; Fu, S.; Schneider, M.D.; et al. Phosphorylation of Thr-178 and Thr-184 in the TAK1 T-loop Is Required for Interleukin (IL)-1-mediated Optimal NF κ B and AP-1 Activation as Well as IL-6 Gene Expression. *J. Biol. Chem.* **2008**, *283*, 24497–24505. [[CrossRef](#)] [[PubMed](#)]
106. Li, R.; Ji, C.; Dai, M.; Huang, J.; Xu, W.; Zhang, H.; Ma, Y. An update on the role of tumor necrosis factor alpha stimulating gene-6 in inflammatory diseases. *Mol. Immunol.* **2022**, *152*, 224–231. [[CrossRef](#)]
107. Singh, U.; Tabibian, J.; Venugopal, S.K.; Devaraj, S.; Jialal, I. Development of an in vitro screening assay to test the antiinflammatory properties of dietary supplements and pharmacologic agents. *Clin. Chem.* **2005**, *51*, 2252–2256. [[CrossRef](#)]
108. Keren-Shaul, H.; Kenigsberg, E.; Jaitin, D.A.; David, E.; Paul, F.; Tanay, A.; Amit, I. MARS-seq2.0: An experimental and analytical pipeline for indexed sorting combined with single-cell RNA sequencing. *Nat. Protoc.* **2019**, *14*, 1841–1862. [[CrossRef](#)]
109. Jaitin, D.A.; Kenigsberg, E.; Keren-Shaul, H.; Elefant, N.; Paul, F.; Zaretsky, I.; Mildner, A.; Cohen, N.; Jung, S.; Tanay, A.; et al. Massively parallel single-cell RNA-seq for marker-free decomposition of tissues into cell types. *Science* **2014**, *343*, 776–779. [[CrossRef](#)]
110. Martin, M. Cutadapt removes adapter sequences from high-throughput sequencing reads. *EMBnet J.* **2011**, *17*, 3. [[CrossRef](#)]
111. Anders, S.; Pyl, P.T.; Huber, W. HTSeq—A Python framework to work with high-throughput sequencing data. *Bioinformatics* **2015**, *31*, 166–169. [[CrossRef](#)] [[PubMed](#)]
112. Love, M.I.; Huber, W.; Anders, S. Moderated estimation of fold change and dispersion for RNA-seq data with DESeq2. *Genome Biol.* **2014**, *15*, 550. [[CrossRef](#)] [[PubMed](#)]
113. Köster, J.; Rahmann, S. Snakemake—A scalable bioinformatics workflow engine. *Bioinformatics* **2018**, *34*, 3600. [[CrossRef](#)]
114. Barrett, T.; Wilhite, S.E.; Ledoux, P.; Evangelista, C.; Kim, I.F.; Tomashevsky, M.; Marshall, K.A.; Phillippy, K.H.; Sherman, P.M.; Holko, M.; et al. NCBI GEO: Archive for functional genomics data sets—Update. *Nucleic Acids Res.* **2012**, *41*, D991–D995. [[CrossRef](#)] [[PubMed](#)]

Disclaimer/Publisher’s Note: The statements, opinions and data contained in all publications are solely those of the individual author(s) and contributor(s) and not of MDPI and/or the editor(s). MDPI and/or the editor(s) disclaim responsibility for any injury to people or property resulting from any ideas, methods, instructions or products referred to in the content.